



An Alternative Approach for the Interpretation of Data from Three-Point Bending of Long Bones

Stavros K. KOURKOULIS¹⁾, Artemis KOUVAKA¹⁾
Chara ANDRIAKOPOULOU¹⁾, Ismene DONTAS²⁾

¹⁾ *National Technical University of Athens
Department of Mechanics, Unit of Biomechanics
Laboratory of Testing and Materials*

Theocaris Building, Zografou Campus, 15773, Athens, Greece
e-mail: stakkour@central.ntua.gr

²⁾ *Laboratory for Research of the Musculoskeletal System “Th. Garofalidis”
School of Medicine, National & Kapodistrian University of Athens
Athens, Greece*

An alternative approach for elaborating the raw data obtained from three-point bending tests of long bones of Wistar rats is described. The aim of the study is to provide mechanical properties of the bone tissue which are independent of the bone geometric characteristics. The study is carried out experimentally *ex vivo*. It is indicated that ignoring the actual shape of the bone's critical cross-section (i.e., the section where fracture occurs) and the inclination of the loading axis with respect to the principal centroidal axes of the critical section, may lead to erroneous results concerning the strength of the tissue.

Key words: three-point bending, long bones, femurs, female Wistar rats, fracture stress.

1. INTRODUCTION

Bending tests (either three- or four-point) are quite often employed in biomechanical studies for the determination of the mechanical response of bones (especially long ones) due to the relatively simple experimental procedure, which permits short exposure time of the specimens. The bending fracture stress (together with the modulus of elasticity and the strain energy absorbed up to fracture) are considered as the most representative quantities for the description of the mechanical behaviour of the specific tissue. Unfortunately, the determination of reduced quantities (like stresses and strains) is not a trivial task in the case

where the specimens are long bones, since these quantities depend on geometric characteristics of the specimen, which are not constant all over its length.

Concerning the stress, it strongly depends on the way the area of the bone's critical cross-section is distributed with respect to the axis of rotation. This dependence is quantified by the second moment of area tensor, \mathbf{I}_{ij} . Moreover, the stress depends on the orientation of the load with respect to the principal centroidal axes ω_p , which in turn depends on the bone tiny anatomic details (dictating the placement of the bone on the supports), on the exact position of the critical point of the section (i.e., the point most distanced from the neutral line of the section), and finally on the possible distance of the loading axis from the centroid of the cross-section (eccentricity), since it dictates the magnitude of shear stresses developed due to the parasitic torsional moments.

In many practical applications, the above problems are usually confronted (or overlooked) by simulating the bone's cross-section either as circular or as elliptic rings [1] of constant thickness. In this study, an alternative approach is described indicating that ignoring the actual shape of the cross-section and the angle between the loading axis and the principal centroidal axes may lead to erroneous results for the tissue's strength.

2. THE EXPERIMENTAL PROTOCOL AND THE RESULTS

The present study is part of a wider research project investigating the possibilities of using plant extracts to cure osteoporosis. Mature (10-month-old) female Wistar rats were used for the experimental protocol, as approved by the General Directorate of Veterinary Services of Greece, according to Greek legislation (Presidential Decree 160/1991), in compliance with the EEC Directive 609/1986. The animals were separated into various groups, allocating littermates to each group, in order to avoid significant genetic and anatomical variations among them. However, in this study the attention is only focused on one of these groups, since the target is to comparatively consider the differences between the various methods for interpreting the raw data of three-point bending tests.

The animals were euthanized with an overdose of ketamine hydrochloride and dexdomitor. Both their right and left femurs were gently dislocated from the tibia and pelvis. The surrounding muscles were carefully removed until the bone was left clear of soft tissues, making sure not to scrape the periosteum. The bones were then wrapped in a sterile gauze dampened with normal saline, closed in sterile urine culture boxes and put in a -10°C freezer until being tested under three-point bending (3PB) conditions.

The experimental set-up included an electromechanical loading frame (10 kN MTS INSIGHT) with a properly calibrated load cell, a video extensometer (RTSS, Limes Messtechnik), a digital photo-camera, suitable grips for 3PB

tests with small specimens, a digital caliper and a personal computer with the appropriate software.

The femurs were placed horizontally on rounded edges of radius of curvature equal to 3 mm at a distance of 20 mm. Attention was paid for all the specimens to be placed (as accurately as possible) in the same manner concerning their orientation in order to minimize scattering factors. The force was applied at the mid-section of the diaphysis (Fig. 1a) using a punch of rounded notch (of radius equal to 3 mm). In Fig. 1b, a typical specimen is shown through the screen of the video extensometer before the onset of the loading procedure.



FIG. 1. Typical specimens: a) while loaded (at the onset of fracturing), b) as it is seen through the screen of the video extensometer before the onset of the loading procedure and c) after the test.

The tests were implemented under displacement-control mode, at a rate equal to 0.5 mm/min, in an effort to simulate quasi-static conditions. The displacement was imposed monotonically and the test was terminated when the fracture of the specimen occurred. The raw data recorded were the applied force (measured with the aid of a calibrated cell of sensitivity equal to 0.1 N) and the deflection of the central section of the specimen, using the video extensometer (distance resolution at 100 mm field of view equal to 0.5 μm). The fracture of all specimens was brittle without any exception at all. A typical fractured specimen is shown in Fig. 1c.

A typical force-deflection curve is shown in Fig. 2, as it is obtained using both the video extensometer and the data provided by the frame software. It is obvious that besides the (expected) initial bedding error characterizing the frame's curve there is a considerable difference in the slope of the two curves: that of the frame's curve is significantly lower. It is thus concluded that the specific way for recording deflection is to be avoided. This rule was followed for all the tests of the present protocol.

In general, the above obtained force-deflection curves are characterized by an initial non-linear portion followed by an almost perfectly linear one. A second non-linear segment always appears before the fracture of the specimens. Beside their similarities some differences appeared also, which dictated the classification

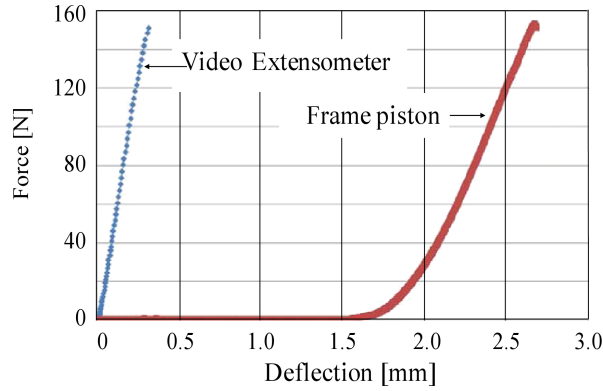


FIG. 2. A load-deflection curve as it was obtained using the data of the video extensometer and also the data of the loading frame software.

of the tests in three categories (shown in Fig. 3). The vast majority of the tests are classified into the first category (Fig. 3a), characterized by the fact that the force-deflection curve is monotonous during the whole duration of the tests. A small number of specimens are classified into the second category (Fig. 3b), including the tests for which after the first cracking of the specimen (denoted by a more or less sudden load-drop) the force kept increasing for a while before the specimen collapsed. Very few specimens were classified in the third category, which includes the tests for which the main force-deflection curve consists of two linear segments (Fig. 3c). The videos of the specific tests revealed that this “discontinuity” was due to an abrupt rotation of the specimen around its longitudinal axis. In the case when the slopes of the two segments of the force-deflection curve were equal to each other, the specimens of the specific category were not excluded from the analysis.

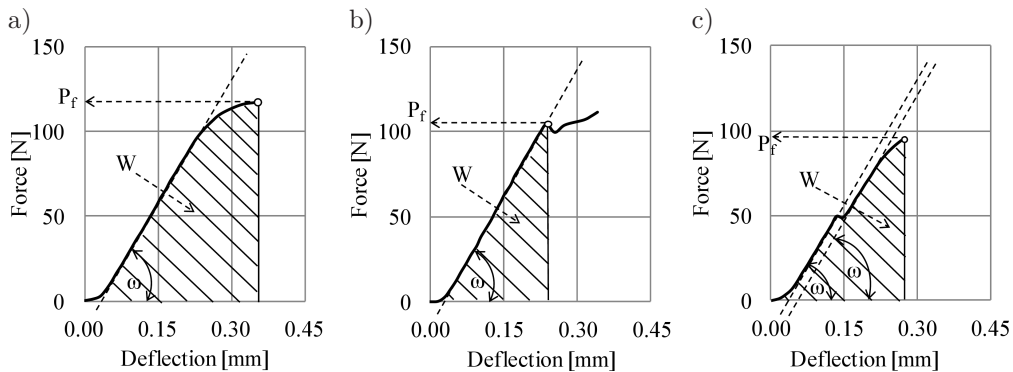


FIG. 3. The three classes of the force-deflection protocol curves recorded during the experimental protocol.

Taking advantage of the force-deflection plots one can determine the peak force P_f [N] sustained by the bone. For the specimens of the first and third categories, P_f was determined as the actual maximum force recorded, while for those of the second category P_f was determined as the force at the first crack (see Fig. 3b). In addition, one can determine the stiffness of the bone [N/mm], quantified as the slope ω of the linear portion of the force-deflection curve and the strain energy W [N · mm], i.e., the energy absorbed by the specimen until the fracture. Since our attention here is focused on the fracture stress, for which only the peak force is required, no details for the determination of the latter quantities (ω , W) are provided. Further analysis of these quantities is given in a forthcoming paper together with data for the other animal groups [2].

3. THE GEOMETRIC CHARACTERISTICS OF THE CRITICAL CROSS-SECTION

Before the implementation of each test, maximum effort was given to accurately define the loading axis. This was achieved by drawing (using permanent red ink) the point where the piston touched the bone's "upper side" and also the point where the loading line intersected the bone's "lower side". This step is crucial since the knowledge of the loading axis permits the analysis of the force along the principal centroidal axes.

After each test, the fractured bone was placed vertically in a small cup (Fig. 4a), which was then filled with molten resin (Fig. 4b). After the appropriate curing period, the resin-bone complex was removed from the cup and its upper surface was polished removing the minimum possible material from the fractured surface until a plane area was obtained. The inner and outer boundaries of the fractured section were thus revealed (Fig. 4c). By using a stereoscope and a digitizer the shape of these two contours was obtained and stored electronically. With the aid of commercially available software, the geometrical

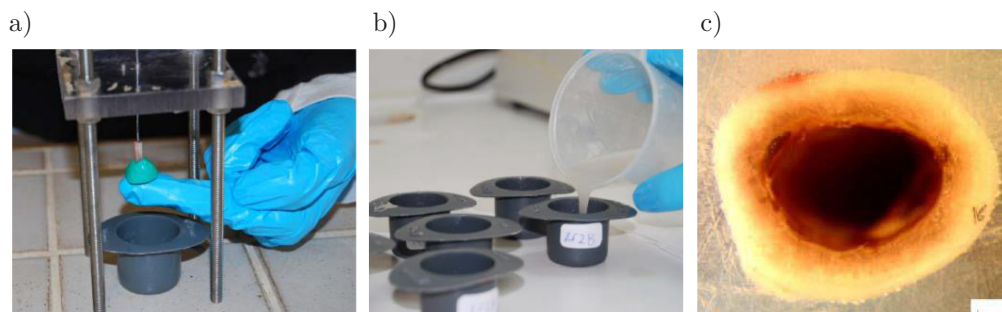


FIG. 4. a) Placing the fractured bone in the cup in vertical position, b) pouring molten resin in the cup, c) the surface of the resin-bone complex after polishing.

features of the fractured cross-section were determined, including (see Fig. 5a): (i) the coordinates of the centroid C , with respect to an arbitrary reference system, (ii) the principal centroidal axes and (iii) the principal second moments of area, (iv) the eccentricity e , i.e., the distance of the centroid from the loading axis, (v) the area of the section A , and (vi) its minimum thickness t . Taking advantage of these data it is possible to determine the fracture stress (using Bernoulli-Euler's technical bending theory considering linearly elastic materials) as follows:

$$(3.1) \quad \sigma_{\text{fracture}} = \frac{P_f L}{4} \left(\pm \frac{\cos |\omega_p| y_m}{I_{z_p z_p}} \pm \frac{\sin |\omega_p| z_m}{I_{y_p y_p}} \right),$$

where L is the span and (y_m, z_m) the critical point (most distanced from the neutral line).

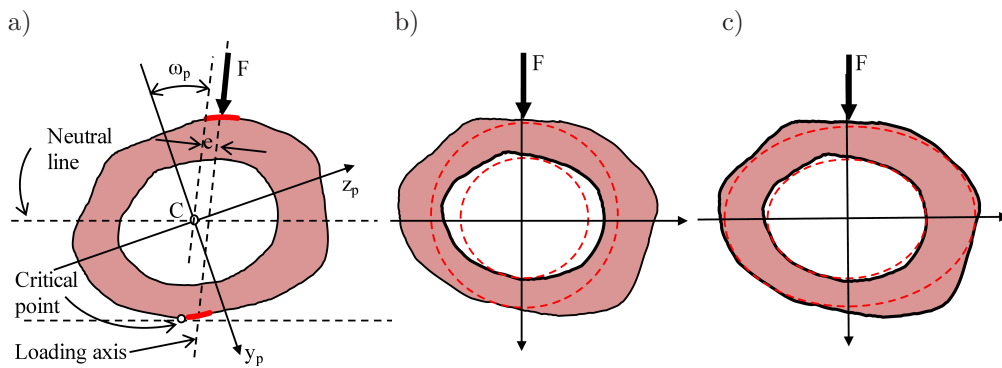


FIG. 5. The quantities required for the determination of normal and shear stresses at the fracture load (Eqs. (3.1) and (3.2)), b) simulating the fractured section as cyclic or c) elliptic-ring.

In addition, one can determine the shear stress developed due to the eccentricity e (assuming that the minimum thickness of the section is relatively small) as follows:

$$(3.2) \quad \tau = \frac{M_t}{2At} = \frac{P_f e}{2At}.$$

4. RESULTS AND CONCLUDING REMARKS

The normal fracture stress, as determined from Eq. (3.1), was compared against the respective one obtained by considering the fractured cross-section either as a circular ring (Fig. 5b) of constant thickness or as an elliptic ring (Fig. 5c) with the load acting normally to the ellipse's major axis. The outer and inner boundaries of these rings were determined using a best-fit procedure,

after a convergence analysis concerning the number of points providing optimum results. The developed parasitic shear stress was also determined from Eq. (3.2). The results are recapitulated in Table 1.

Table 1. Bending fracture stress and the respective parasitic shear stress in MPa.

Present approach	Circular ring	Elliptic ring	<i>Parasitic shear stress</i>
170.3	160.5	187.4	10.6

It is concluded that ignoring the actual geometric details of the cross-section results in differences for the fracture stress varying between 5% and 13%. The differences of this order (although well affordable in some experimental protocols) could be proven crucial, in case, for example, of comparative studies that are implemented for the assessment of various pharmaceutical treatments [3]. Moreover, the parasitic shear stresses of the order of 6% of the respective normal ones are by no means to be ignored.

REFERENCES

1. SAFFAR K.P., JAMILPOUR N., RAJAAI S.M., *How does the bone shaft geometry affect its bending properties?*, American Journal of Applied Sciences, **6**(3): 463–470, 2009.
2. KOURKOULIS S.K., DONTAS I., KOUVAKA A., ANDRIAKOPOULOU CH.H., *Biomechanical analysis of three point bending tests of long bones*, to be submitted, 2016.
3. KOURKOULIS S.K., ANDRIAKOPOULOU CH.H., KOUVAKA A., *Three-point bending of long bones: Accurate calculation of the fracture stress* [in Greek], Proceedings of the 5th International Conference of the Hellenic Society on Biomechanics, Thessaloniki, Greece, Paper Code: O-24, 2012.

Received October 13, 2016; accepted version October 18, 2016.
